

$V'Z$ and $V'W$ production as tests of heavy gauge boson couplings at future hadron colliders

Mirjam Cvetič and Paul Langacker

Department of Physics, University of Pennsylvania, Philadelphia, Pennsylvania 19104-6396

(Received 8 July 1992)

We point out that the production cross section of $pp \rightarrow V'V$, with $V' = W', Z'$ and $V = W, Z$, is a useful diagnostic of V' gauge couplings at future hadron colliders. For $M_{Z'} \approx 1$ TeV it would allow determination of combinations of Z' gauge couplings to the quarks to around 10%. An analysis of the extraction of gauge couplings from the complementary tests—forward-backward asymmetry, rare decays $pp \rightarrow V' \rightarrow f_1 \bar{f}_2 V$, and the production cross section $pp \rightarrow V'V$ —is given in a model-independent framework. Four ratios of charges are needed to characterize a general gauge theory with an additional family-independent $U(1)$ factor. We show that there are four functions of these ratios observable at hadron colliders, but for projected Superconducting Super Collider and Large Hadron Collider luminosities only two combinations can be extracted. These yield a significant discrimination between interesting grand-unified-theory-motivated models. Clean tests of whether a new W' couples to right-handed currents, of the ratio g_R/g_L of gauge couplings, and of the non-Abelian vertex in left-right-symmetric models are described.

PACS number(s): 12.15.Cc, 12.10.Dm, 13.85.Qk, 14.80.Er

I. INTRODUCTION

Extended gauge structures are an essential part of grand unification. In string theory the gauge group at the compactification scale is generally larger than that of the standard model. Although there is no *a priori* reason (except in some cases of restrictive particle representation) to constrain the mass of the new gauge boson to the accessible range of a few TeV, the existence of new gauge bosons in this energy range is a plausible consequence of a number of types of new physics [1].

Current limits on extra neutral gauge bosons (Z') are relatively weak. The analysis of Z -pole, weak neutral current, and collider data puts lower bounds [2–5] on the masses of various types of Z' 's in the range of 160–400 GeV, with stronger limits around 500–1000 GeV in some specific models in which the mass and the Z - Z' mixing angle are related.

The limits on the new charged gauge bosons W'^{\pm} are more constrained in specific models; in particular, in the left-right-symmetric models [6] based on the extended gauge structure $SU(2)_L \times SU(2)_R \times U(1)_{B-L}$. For the models with $g_L = g_R$ [respective gauge couplings for $SU(2)_L$, $SU(2)_R$] and equal magnitude of the left-handed and right-handed quark mixing matrix elements, the bound on the mass of the heavy charged W' is $M_{W'} > 1.4$ TeV, based on the K_S - K_L mass difference [7], and the W - W' mixing angle is $|\theta_+| < 0.003$ from universality [8]. For general left-right-symmetric models these bounds are much weaker [9]: $g_L M_{W'}/g_R > 300$ GeV and $g_R |\theta_+|/g_L < 0.013$. Stronger limits follow from CP violation unless there is fine tuning [10].

On the other hand, the Z' can be produced [11,4] (and clearly detected via leptonic decays) at the Large Hadron Collider (LHC) and Superconducting Super Collider (SSC) if its mass does not exceed around 5 TeV [11–14].

The immediate goal after the discovery of a new gauge

boson would be to try to understand its origin and properties [15]. Subsequent tests should be able to address and separate the following: (i) The nature of the gauge couplings of new gauge bosons to ordinary fermions, including the pattern of charges for a new Z' , whether a new W' couples to $V+A$ currents, and the overall strength of the gauge coupling; (ii) the nature of the symmetry-breaking structure; and (iii) the coupling of the gauge bosons to exotic fermions and supersymmetric partners.

Although the three phenomena are interconnected, the aim is to study experimental signals that can separate them. Some aspects of the nature of symmetry breaking structure, in particular, the decays $V' \rightarrow VV$ ($V = W, Z$; $V' = W', Z'$) [16–19] and the $M_{W'}/M_{Z'}$ mass ratio [1,20], as well as the study of decays of V' into exotic fermions [21], have been studied earlier.

In this paper we address the diagnostic study of the gauge couplings. One immediate possibility is the measurement of $\sigma(pp \rightarrow V')B$, where $\sigma(pp \rightarrow V')$ is the total production cross section and B is the branching ratio into leptons. σ could be calculated for a given set of (Z' , W'^{\pm}) couplings to within a few percent. However, the theoretical branching ratio $B \equiv \Gamma(Z' \rightarrow l^+ l^-)/\Gamma_{\text{tot}}$, where $l = (e, \mu, \text{ or both})$ and Γ_{tot} is the total width, with an analogous definition for W' , is model dependent because it depends on the contribution of exotic fermions and supersymmetric partners to the V' width. These could easily change σB by a factor of 2. Thus σB cannot be useful as a diagnostic test for the V' gauge coupling; however, it would be a useful indirect probe for the existence of the exotic fermions or superpartners.

On the other hand, from measurements of the total width [14] Γ_{tot} , which could be determined from the line shape of $Z' \rightarrow l^+ l^-$, and σB one obtains $\sigma \Gamma(Z' \rightarrow l^+ l^-) \equiv \sigma B \Gamma_{\text{tot}}$. This probes the absolute magnitude of the gauge couplings in the combination

$g_2^4 [a(\hat{g}_{L2}^{u2} + \hat{g}_{R2}^{u2}) + b(\hat{g}_{L2}^{d2} + \hat{g}_{R2}^{d2})](\hat{g}_{L2}^{f/2} + \hat{g}_{R2}^{f/2})$, where \hat{g}_{L2}^f (\hat{g}_{R2}^f) is the charge of the left (right)-handed fermion f , g_2 is the gauge coupling of the new boson, and a and b are calculable coefficients that depend on the V' mass, the c.m. energy, and the proton structure functions. The charges are characteristic of the gauge group. Once this is identified (as described below), $\sigma B \Gamma_{\text{tot}}$ would determine the gauge coupling g_2 , which is a useful probe of the pattern of spontaneous symmetry breaking in grand unified theories (GUT's) [22] and left-right-symmetric models.

The production cross section for $pp \rightarrow V'g$, with g a gluon, has a large rate but is not a useful probe. It has the same branching ratio uncertainties as σB . Furthermore, since gluons couple to the vector component of fermionic currents, this process measures the same combination of gauge couplings as $\sigma(pp \rightarrow V')$, so that the ratio of cross sections yields no new information.

In this paper we propose [23] the cross section $pp \rightarrow V'V$ as a useful probe [25], since it measures a different combination of couplings: $g_1^2 g_2^2 (\hat{g}_{L1}^q \hat{g}_{L2}^q + \hat{g}_{R1}^q \hat{g}_{R2}^q)$. Here g_1 and g_2 are the gauge coupling constants of the V and V' , respectively, while $\hat{g}_{(L,R)1}^q$ and $\hat{g}_{(L,R)2}^q$ are the corresponding charges of the (left,right)-handed quarks. In this case the uncertainty due to the exotics and g_2 is removed by dividing the production rate by that for $pp \rightarrow V'$. For leptonic decays of $Z' \rightarrow e^+e^-$ ($\mu^+\mu^-$) and (Z, W) decaying into either leptons or quarks this process is virtually free of backgrounds. The rate is sufficient to give good statistics for $M_{V'} \sim 1$ TeV and provides a diagnostic test for the gauge coupling of V' to quarks.

This is complementary to the rare decays [26] recently proposed [24] and studied in detail [24,27,28] as a useful diagnostic of the heavy gauge boson couplings to the ordinary fermions. Such rare decays involve $V' \rightarrow f_1 \bar{f}_2 V$, where $F_{1,2}$ are ordinary fermions. For $V=Z$ the combination $g_1^2 g_2^2 (\hat{g}_{L1}^2 \hat{g}_{L2}^2 + \hat{g}_{R1}^2 \hat{g}_{R2}^2)$ is measured, while for $V=W$, such decays project out \hat{g}_{L2} couplings. Although the rates are suppressed by a factor of $\alpha/2\pi$ compared with $V' \rightarrow f_1 \bar{f}_2$, they have a logarithmic enhancement proportional to $\ln^2(M_{V'}/M_V^2)$, closely related to collinear and infrared singularities of QED [29,30]. The gold-plated events (free of major backgrounds) turn out to be [24] $Z' \rightarrow W e \bar{\nu}_e (\mu \bar{\nu}_\mu)$. Dividing by the $Z' \rightarrow l^+ l^-$ rate one has a clean test of the coupling of Z' to leptons. In addition, the absence of $W'^{\pm} \rightarrow W^{\pm} e^+ e^- (\mu^+ \mu^-)$ is an excellent test of the right-handedness of the W' .

The third clean probe for gauge couplings is the forward-backward asymmetry A_{FB} [11] for the process $pp \rightarrow Z' \rightarrow e^+e^-$ or $\mu^+\mu^-$. It can distinguish between different models for $M_{Z'}$, up to a few TeV, and tests a combination of the couplings of Z' to quarks and leptons.

This paper is organized as follows. In Sec. II the formalism and the models used in the calculation are described. The major part of the paper, Sec. III involves a study of the proposed production cross sections $pp \rightarrow V'V$, with definitions of appropriate ratios and backgrounds. In Sec. IV we discuss the extraction of detailed information about the gauge couplings. We point out how to study family universality, the nature of the

enhanced gauge symmetry, and the values of the gauge couplings for particular fermions based on the above three diagnostic probes. We show that considerable diagnostic information can be obtained in hadron colliders. Conclusions are given in Sec. V.

II. FORMALISM

The neutral-current gauge interaction term in the presence of an additional U(1) can be written as

$$-L_{\text{NC}} = e J_{\text{em}}^\mu A_\mu + g_1 J_1^\mu Z_{1\mu} + g_2 J_2^\mu Z_{2\mu}, \quad (2.1)$$

with Z_1 being the $\text{SU}(2) \times \text{U}(1)$ boson and Z_2 the additional boson in the weak eigenstate basis. Here $g_1 \equiv (g_L^2 + g_Y^2)^{1/2} = g_L / \cos\theta_W$, where g_L , g_Y are the gauge couplings of $\text{SU}(2)_L$ and $\text{U}(1)_Y$, and g_2 is the gauge coupling of Z_2 . The GUT-motivated cases have $g_2 = \sqrt{5/3} \sin\theta_W g_1 \lambda_g^{1/2}$, where λ_g depends on the symmetry-breaking pattern [22]. If the GUT group breaks directly to $\text{SU}(3) \times \text{SU}(2) \times \text{U}(1) \times \text{U}'(1)$ then $\lambda_g = 1$.

The currents in (2.1) are

$$J_j^\mu = \frac{1}{2} \sum_i \bar{\psi}_i \gamma^\mu [\hat{g}_{Vj}^i - \hat{g}_{Aj}^i \gamma_5] \psi_i, \quad j=1,2, \quad (2.2)$$

where the sum runs over fermions, and the $\hat{g}_{(V,A)j}^i$ correspond to the vector and axial-vector couplings of Z_j to i th flavor. Analogously, $\hat{g}_{(L,R)j}^i = \frac{1}{2}(\hat{g}_{Vj}^i \pm \hat{g}_{Aj}^i)$, so that $\hat{g}_{L1}^i = t_{3L}^i - \sin^2\theta_W q^i$ and $\hat{g}_{R1}^i = -\sin^2\theta_W q^i$, where t_{3L}^i and q^i are, respectively, the third component of weak isospin and electric charge of fermion i . We will illustrate our study of Z_2 currents with the following GUT, left-right (LR), and superstring-motivated models:

- (i) Z_χ occurs in $\text{SO}(10) \rightarrow \text{SU}(5) \times \text{U}(1)_\chi$.
- (ii) Z_ψ occurs in $\text{E}_6 \rightarrow \text{SO}(10) \times \text{U}(1)_\psi$.
- (iii) $Z_\eta = \sqrt{3}/8 Z_\chi - \sqrt{5}/8 Z_\psi$ occurs in superstring-inspired models in which E_6 breaks directly to a rank 5 group.
- (iv) The general E_6 boson $Z(\beta) = \cos\beta Z_\chi + \sin\beta Z_\psi$, where $0 \leq \beta < \pi$ is a mixing angle. The Z_χ , Z_ψ , and Z_η are special cases with $\beta=0, \pi/2$ and

$$Z_\eta = Z(\beta = \pi - \arctan\sqrt{5/3}),$$

respectively.

- (v) Z_{LR} occurs in left-right symmetric models, where the ratio $\kappa = g_R/g_L$ of the gauge couplings $g_{L,R}$ for $\text{SU}(2)_L$, $\text{SU}(2)_R$ respectively, parametrizes the whole class of models. In this case $\lambda_g = 1$ by construction and $\kappa > 0.55$ for consistency [20].

(vi) Z'' has the same couplings as the ordinary Z ; it cannot occur in extended gauge theories, but could occur in composite models. It is a useful reference point for comparing the sensitivity of experimental signals. Note, however, that the more realistic cases (i)–(v) have weaker couplings to the ordinary fermions. The chiral couplings $\hat{g}_{(L,R)}$ for specific models are given in Ref. [5] but are repeated for convenience in Table I.

III. VV' PRODUCTION CROSS SECTIONS

Heavy neutral gauge bosons Z' can be produced at future hadron colliders (SSC and LHC) and can be detected

TABLE I. Couplings of the Z_χ , Z_ψ , and Z_η to a 27-plet of E_6 . The SO(10) and SU(5) representations are also indicated. The couplings are shown for the left-handed (L) particles and antiparticles. The couplings of the right-handed particles are minus those of the corresponding L antiparticles. The D is an exotic SU(2) singlet quark with charge $-\frac{1}{3}$. $(E^0, E^\pm)_{L,R}$ is an exotic lepton doublet with vector SU(2) couplings. N and S are new Weyl neutrinos that may have large Majorana masses. The Z_{LR} couples to the charge $\sqrt{3}/5[\beta T_{3R} - 1/(2\beta)T_{B-L}]$, where $\beta = (\kappa^2 \cot^2 \theta_W - 1)^{1/2}$ and $\kappa = g_R/g_L$.

SO(10)	SU(5)	$2\sqrt{10}Q_\chi$	$\sqrt{24}Q_\psi$	$2\sqrt{15}Q_\eta$
16	$10 (u, d, \bar{u}, e^+)_L$	-1	1	-2
	$5^* (\bar{d}, \nu, e^-)_L$	3	1	1
	$1\bar{N}_L$	-5	1	-5
10	$5 (D, \bar{E}^\sigma, E^+)_L$	2	-2	4
	$5^* (\bar{D}, E^0, E^-)_L$	-2	-2	1
1	$1S_L^0$	0	4	-5

via the resultant leptonic decays $pp \rightarrow Z' \rightarrow e^+e^-(\mu^+\mu^-)$, and the charged gauge bosons $W^{\pm'}$ are detected via the modes [31] $pp \rightarrow W^{\pm'} \rightarrow \bar{l}n_l(l\bar{n}_l)$, where n_l is a right-handed neutrino. For given Z' couplings the total cross section $\sigma(pp \rightarrow Z')$ can be computed quite accurately, since the quark cross section and distribution functions are known up to $O(\alpha_s)$. The cross sections are given in Refs. [11–14]. In the following we assume (for illustration) leptonic branching ratios B corresponding to decays into 16-plets for Z_χ and Z_{LR} , 27-plets for Z_ψ and Z_η , and 15-plets for Z'' , and no superpartners.

Neutral weak eigenstates Z_1 and Z_2 can be identified with the mass eigenstates Z and Z' , respectively, because the Z - Z' mixing is negligible, as suggested from gauge theories as well as experiment [2–5]. The squared amplitude [see Fig. 1(a) and Fig. 1(b) for the Feynman diagrams] for the quark process $q\bar{q} \rightarrow Z'Z$ averaged

(summed) over initial (final) polarizations can be written as [32]

$$\mathcal{M}_{Z,Z'} = 16\pi \frac{d\sigma}{d\hat{t}} = 2 \frac{C_{ffZ}}{\hat{s}^2} \left\{ \left[\frac{\hat{t}}{\hat{u}} + \frac{\hat{u}}{\hat{t}} \right] + 2 \frac{m_+}{\hat{u}\hat{t}} - m_1 m_2 \left[\frac{1}{\hat{u}^2} + \frac{1}{\hat{t}^2} \right] \right\}, \quad (3.1)$$

where $C_{ffZ} = g_1^2 g_2^2 (\hat{g}_{L1}^{q2} \hat{g}_{L2}^{q2} + \hat{g}_{R1}^{q2} \hat{g}_{R2}^{q2})$; \hat{s} , \hat{t} , and \hat{u} are the Mandelstam variables; $\hat{u} = \hat{u}/\hat{s}$, $\hat{t} = \hat{t}/\hat{s}$; $m_{1,2} = M_{1,2}^2/\hat{s}$; $m_\pm = m_1 \pm m_2$; and $M_{1,2}$ are the respective masses for Z, Z' . The total quark cross section is

$$\sigma = \int_{\hat{t}_{\min}}^{\hat{t}_{\max}} \frac{d\sigma}{d\hat{t}} d\hat{t} = \frac{C_{ffZ}}{4\pi\hat{s}} \left\{ \frac{1+m_+^2}{1-m_+} \ln \frac{1-m_+ + \beta}{1-m_+ - \beta} - 2\beta \right\}, \quad (3.2)$$

where $\hat{t}_{\min, \max} = \frac{1}{2}\hat{s}\{m_+ - 1 \pm \beta\}$, and $\beta = (1 - 2m_+ + m_-^2)^{1/2}$.

In $U'(1)$ gauge theories one has $[Q', T_i] = 0$. Then, neglecting mixing, the same formulas (3.1) and (3.2) apply to $q_1\bar{q}_2 \rightarrow Z'W$, with the appropriate replacements of the gauge couplings and the W mass. Here, Q' is the generator of $U'(1)$ and the T_i 's are the $SU(2)_L$ generators.

On the other hand, in theories with mixing the effective $\hat{g}_{L2}^{q1} \neq \hat{g}_{L2}^{q2}$. The \hat{t} and \hat{u} channel fermion exchange contributions become more complicated, and there is also another contribution from the non-Abelian graph [see Fig. 1(c)] due to the $Z'Z$ mixing $\propto \theta_{Z'Z}$, which is responsible for the restoration of unitarity. Thus, formulas (3.1) and (3.2) are not strictly correct in this case. However, in gauge theories with $M_2 \gg M_1$ and small Z - Z' mixing (as constrained from experiments) [33] $(\hat{g}_{L2}^{q1} - \hat{g}_{L2}^{q2}) \sim \theta_{Z'Z} \propto (\hat{g}_{L2}^{q1})M_1^2/M_2^2$. Note also that $M_1^2 \ll M_2^2 \leq \hat{s}$ is the limit in which unitarity should be restored. It can then be shown, using related formulas to those [32] for ZW production in the standard model, that (3.1) is still valid in the leading order $(\hat{g}_{L2}^{q1} - \hat{g}_{L2}^{q2}) = (\hat{g}_{L2}^q)$; the correction is suppressed by a factor of $(\theta_{Z'Z}/\hat{g}_{L2}^q)^2 M_2^2/M_1^2 \propto M_1^2/M_2^2$, and is thus negligible. However, in compositeness-motivated theories [e.g., model (vi) with Z''] the gauge invariance need not be restored; in this case the analogues (3.1) and (3.2) violate unitarity. In such models the rare decays $Z' \rightarrow f_1\bar{f}_2 W$ also have anomalous rates in violation of unitarity [24].

In models with heavy charged gauge bosons W' the production cross sections for the processes $q\bar{q} \rightarrow W'W$ can be evaluated using formulas (3.1) and (3.2), with the corresponding values of the gauge couplings and masses, provided one neglects WW' mixing. Since $q\bar{q} \rightarrow W'W$ directly probes the $(\hat{g}_{L2}^f)^2$, it should be strongly suppressed (by the square of the W - W' mixing angle or by $m_f^2/M_{W'}^2$) in the left-right-symmetric models. Absence of such events would thus provide a good check that the coupling of W' is right handed. This is a second independent check of the right handedness of W' , the first being

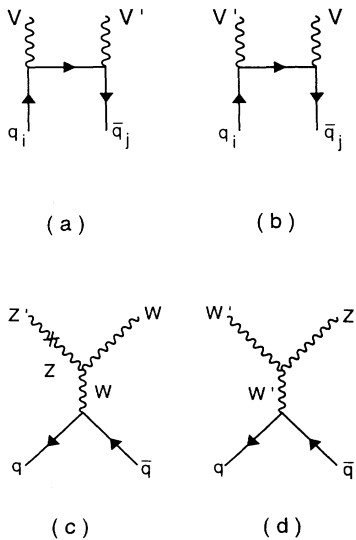


FIG. 1. (a) and (b) Lowest-order diagrams for $q_i \bar{q}_j \rightarrow VV'$. (c) Additional non-Abelian diagram for $q\bar{q} \rightarrow Z'W$ induced by Z - Z' mixing. (d) Non-Abelian diagram for $q\bar{q} \rightarrow W'Z$, which is present even in the absence of mixing.

the absence of rare decays $pp \rightarrow W' \rightarrow f\bar{f}W$ [24].

The second process with a heavy charged W' involves the production cross section for $q_i\bar{q}_j \rightarrow W'Z$. In this process the non-Abelian vertex [see Fig. 1(d)] $W'W'Z$ is im-

portant even in the absence of mixing; i.e., it is not suppressed by M_1^2/M_2^2 . In the left-right-symmetric models the squared amplitude for this process is of the form [32]

$$\mathcal{M}_{W'Z} = 16\pi \frac{d\sigma}{d\hat{t}} = 2 \frac{g_1^2 g_R^2 (\hat{g}_{R2}^q)^2}{\hat{s}^2} \left\{ \left[\frac{\rho_{W'Z}}{1-m_2} \right]^2 A + \frac{2\rho_{W'Z}}{1-m_2} [-\hat{g}_{R1}^i I(t) + \hat{g}_{R1}^j I(u)] \right. \\ \left. + (\hat{g}_{R1}^i - \hat{g}_{R1}^j)^2 E + (\hat{g}_{R1}^i)^2 \frac{\gamma}{\tilde{u}^2} + 2\hat{g}_{R1}^i \hat{g}_{R1}^j \frac{m_+}{\tilde{u}\tilde{t}} + (\hat{g}_{R1}^j)^2 \frac{\gamma}{\tilde{t}^2} \right\}, \quad (3.3)$$

with

$$A = \frac{1}{m_1 m_2} \left[\frac{\gamma}{4} (1 - 2m_+ + 3m_+^2 - 2m_-^2) \right. \\ \left. + \frac{m_+}{2} (1 - 2m_+ + m_-^2) \right], \\ I(t) = \frac{1}{m_1 m_2} \left[\frac{\gamma}{4} \left(1 - m_+ - \frac{m_+^2 - m_-^2}{\tilde{t}} \right) \right. \\ \left. + \frac{m_+}{2} \left(1 - m_+ + \frac{m_+^2 - m_-^2}{2\tilde{t}} \right) \right], \quad (3.4) \\ E = \frac{1}{m_1 m_2} \left[\frac{\gamma}{4} + \frac{m_+}{2} \right].$$

Here $\gamma = \tilde{t}\tilde{u} - m_1 m_2$. The quantities \tilde{u} , \tilde{t} , $m_{1,2}$, and m_{\pm} are defined after Eq. (3.1) with $M_1 = M_Z$ and $M_2 = M_{W'}$. The couplings $\hat{g}_{R1}^{i,j}$ and \hat{g}_{R2}^q are the corresponding charges for (i,j) quark couplings to Z and W' , respectively, while $g_1 \rho_{W'Z}$ corresponds to the strength of the $W'W'Z$ non-Abelian vertex. In the left-right-symmetric model one expects $\rho_{W'Z} = \mp \sin^2 \theta_W$ for W'^{\pm} , respectively. Note that this process not only provides a way to measure the strength of the right-handed W' coupling but is also a test of the non-Abelian vertex $W'W'Z$.

The total production cross section $\sigma_{V'V}$ for the above processes is obtained in a straightforward manner using the quark distribution functions of Ref. [34]. This cross section is compared with the basic process $pp \rightarrow Z' \rightarrow l^+ l^-$ by defining the ratios

$$R_{Z'V} = \frac{\sigma(pp \rightarrow Z'V)B(Z' \rightarrow l^+ l^-)}{\sigma(pp \rightarrow Z')B(Z' \rightarrow l^+ l^-)}, \quad (3.5)$$

with $V = Z$ or W decaying into leptons or quarks. We define the cross section for $pp \rightarrow Z'W$ as the sum over W^+ and W^- . In the models with heavy charged gauge bosons the ratios

$$R_{W'V} = \frac{\sigma(pp \rightarrow W'V)B(W' \rightarrow l\bar{n}_l + \bar{l}n_l)}{\sigma(pp \rightarrow W')B(W' \rightarrow l\bar{n}_l + \bar{l}n_l)} \quad (3.6)$$

can be defined analogously. The branching ratios involve decay modes with charged leptons, which provide clean signals, especially for Z' .

In Figs. 2(a) and 2(b) we plot the ratios $R_{Z'W}$ and $R_{Z'Z}$ as a function of the Z' mass along with typical statistical

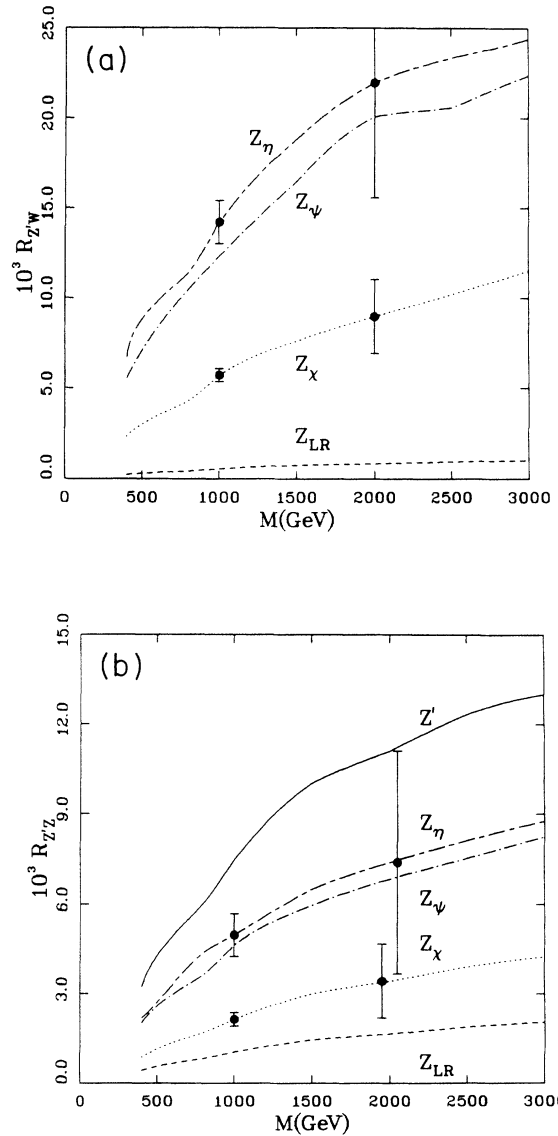


FIG. 2. The ratios (a) $R_{Z'W}$ and (b) $R_{Z'Z}$ as a function of the Z' mass along with typical statistical error bars for the Z_χ , Z_ψ , Z_η , and Z_{LR} for a one year (10^7 s) run at the LHC with a projected luminosity 10^{34} $\text{cm}^2 \text{s}^{-1}$. For the SSC the $R_{V'V}$ are around 20% higher.

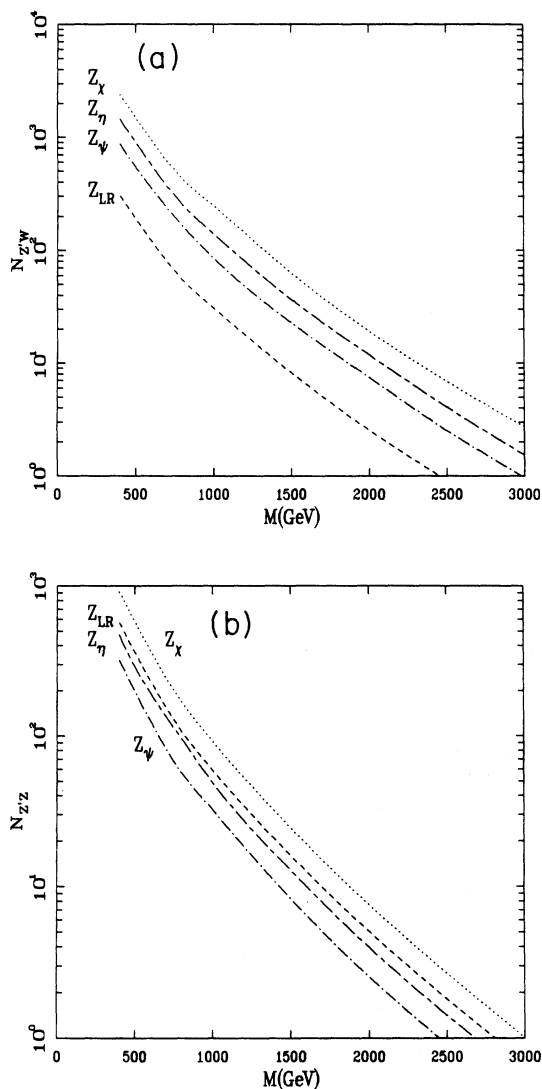


FIG. 3. The numbers of events (a) $N_{Z'W}$ and (b) $N_{Z'Z}$ for $pp \rightarrow Z'V$ and $Z' \rightarrow l^+l^-$, $l = e$ or μ (summed), assuming a one-year run at the LHC.

error bars for a one year (10^7 s) run at the LHC (projected luminosity 10^{34} $\text{cm}^{-2}\text{s}^{-1}$). The error bars are estimated using the total number of $Z'V$ events shown in Figs. 3(a) and 3(b). These assume the specific branching ratios described above, and are presented only for illustration. The R values themselves are independent of the number of exotic decay channels. The production cross sections $pp \rightarrow V'$ are presented in Refs. [11–14]. The R 's increase with the V' mass, but the statistical error bars are too

large for $M_{Z'} \geq 2$ TeV for the measurement to be useful. For the projected SSC luminosity of 10^{33} $\text{cm}^{-2}\text{s}^{-1}$ there are roughly half as many $V'V$ events for $M_{Z'} \leq 1$ TeV and equal numbers for $M_{Z'} > 2$ TeV. The R values are typically 20% larger for the SSC. This is an example in which increased luminosity would significantly improve the statistics, and thus allow one to study the properties of new gauge bosons in a higher mass range.

In the following we study the sensitivity of the R 's for different models with $M_{Z'} = 1$ TeV at the LHC. In Table II the values of $R_{Z'W}$ and $R_{Z'Z}$ are given for different models along with their statistical error bars. The formula (3.1) does not apply to the Z'' for $R_{Z'W}$ because $\hat{g}_{L2}^u \neq \hat{g}_{L2}^d$; however, Eq. (3.3) can be used with appropriate changes for the masses and gauge couplings without the contribution of the non-Abelian graph. Clearly, such an amplitude badly violates unitarity. For comparison the values of the ratio $r_{l\nu W} = B(Z' \rightarrow l\nu W) / B(Z' \rightarrow l^+l^-)$ of the gold-plated rare decay $Z' \rightarrow l\nu W$ (see Fig. 4 for the corresponding Feynman diagram), as well as the forward-backward asymmetry A_{FB} , are given along with their statistical error bars. The statistical errors for the R 's are slightly larger than those of $r_{l\nu W}$ and the forward-backward asymmetry, but are still sufficiently small for $M_{Z'} = 1$ TeV and the projected LHC luminosity. In the case of Z_ψ and Z_η the error bars are too large to distinguish between the two models.

In Fig. 5 the $R_{Z'V}$'s are plotted as a function of $\cos\beta$ for the model (iv) with $Z(\beta)$, and the estimated error bars are displayed. Again, the $R_{Z'V}$'s are a sensitive probe of these models, although there are clearly ambiguities.

In Fig. 6 the $R_{Z'V}$'s are plotted as a function of κ for the left-right models (v) along with typical error bars. The $R_{Z'V}$'s are sensitive functions of κ , especially in the interesting region $\kappa < 1.1$, and could provide a measurement of κ independent of measurements from $r_{l\nu W}$ and A_{FB} .

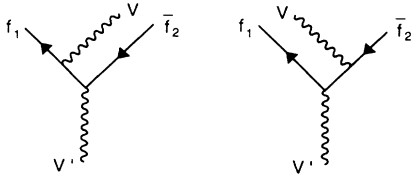
In Fig. 7 is plotted the predictions for $R_{Z'W}$ versus $R_{Z'Z}$ for the χ , ψ , η , and LR ($\kappa = 1$) models, along with expected bars for $M_{Z'} = 1$ TeV.

In Fig. 8 the ratio $R_{W'Z}$ [defined in (3.6)] is shown for W' in the left-right-symmetric model as a function of $M_{W'}$ for the LHC and SSC. This is an absolute prediction of the model and is a sensitive test of both the right-handed W' coupling (independent of the test from the nonobservation of $pp \rightarrow W'W$), but also of the non-Abelian $W'W'Z$ vertex.

We now discuss backgrounds. $Z'V$ production, with Z' subsequently decaying into charged leptons and V into hadrons, charged leptons, or missing neutrinos, are clean events without major standard-model backgrounds. $W'V$

TABLE II. Ratios $R_{Z'V}$, $r_{l\nu W}$, and A_{FB} with their error bars at the LHC for $M_{Z'} = 1$ TeV for the models described in the text.

	Z_χ	Z_ψ	Z_η	Z_{LR}	Z''
$R_{Z'Z}$	0.0021 ± 0.0002	0.0046 ± 0.0008	0.0050 ± 0.0007	0.0010 ± 0.0001	0.0071 ± 0.0003
$R_{Z'W}$	0.0057 ± 0.0004	0.012 ± 0.001	0.014 ± 0.001	0.0005 ± 0.0001	0.310 ± 0.002
$r_{l\nu W}$	0.055 ± 0.0014	0.030 ± 0.002	0.012 ± 0.001	0.022 ± 0.0008	0.26 ± 0.002
$A_{\text{FB}}^{e^+e^-}$	-0.134 ± 0.007	0.000 ± 0.016	-0.025 ± 0.014	0.100 ± 0.006	0.045 ± 0.004

FIG. 4. Diagrams for $V' \rightarrow V f_1 \bar{f}_2$.

productions with W' decaying to ln_l would be very clean if the n_l is heavy and decays in the detector. Otherwise, there could in principle be a standard-model background from $pp \rightarrow WV$ with $W \rightarrow lv_l$. However, this background can be cleanly eliminated at a loss of only a few percent of the signal by requiring the transverse mass m_{Tln_l} of the ln_l system to be larger than 90 GeV.

The calculations here utilize the lowest-order expressions in Eqs. (3.1), (3.2), and (3.3) for the cross section and the quark C distribution functions in Ref. [34]. Of course, if a heavy V' were actually observed, the calculations would have to be redone using up-to-date distributions and including $O(\alpha_s)$ QCD corrections.

IV. EXTRACTING INFORMATION FROM EXPERIMENTAL DATA

We have three types of independent experimental signals: (i) the forward-backward asymmetry A_{FB} [11], (ii) the rare decays $pp \rightarrow V' \rightarrow f_1 \bar{f}_2 V$ [26,24], and (iii) the production cross section $pp \rightarrow V' V$, which provide useful complementary probes to extract information about the nature of the gauge couplings. When expressed in terms of appropriate ratios all are independent of uncertainties from Γ_{tot} and the overall coupling strength g_2 .

In this chapter we present a systematic and model-independent approach for extracting information con-

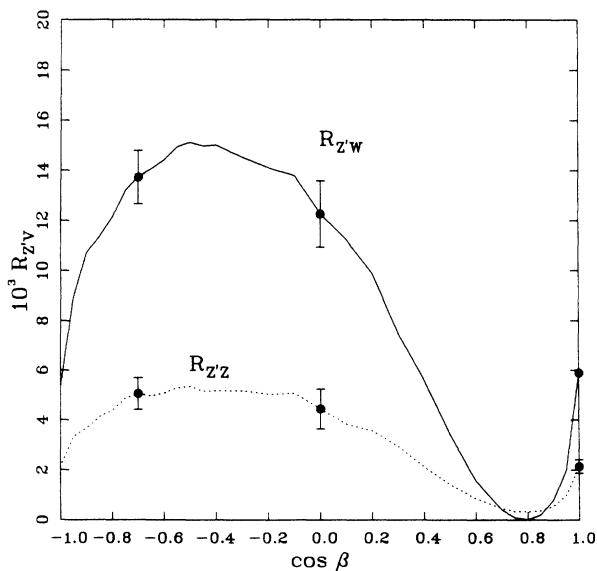


FIG. 5. The ratios R plotted as a function of $\cos\beta$ for the general E_6 boson $Z(\beta) = \cos\beta Z_\chi + \sin\beta Z_\psi$. The error bars are for the LHC with $M_{Z'} = 1$ TeV.

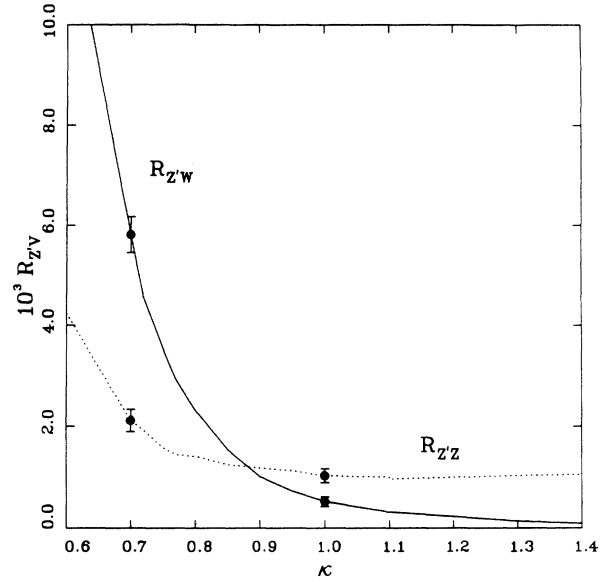


FIG. 6. The ratios R plotted as a function of $\kappa = g_R/g_L$. The error bars are for the LHC with $M_{Z'} = 1$ TeV.

cerning the gauge couplings of the quarks and leptons from the above experimental signals. We will generally assume that the couplings of the new Z' are family universal, that the extended gauge group commutes with the standard model (i.e., $[Q', T_{iL}] = 0$), and that Z - Z' mixing can be ignored. However, we will first comment on the possibility of actually testing these assumptions.

Interfamily universality. The signals that would most clearly test the e - μ family universality are the branching ratios for $B(Z' \rightarrow e^+e^-)$ versus $B(Z' \rightarrow \mu^+\mu^-)$. In order to test the third-family universality, the measurement of the branching ratio $B(Z' \rightarrow \tau^+\tau^-)$ is needed. In spite of having missing neutrinos in the dominant decay mode

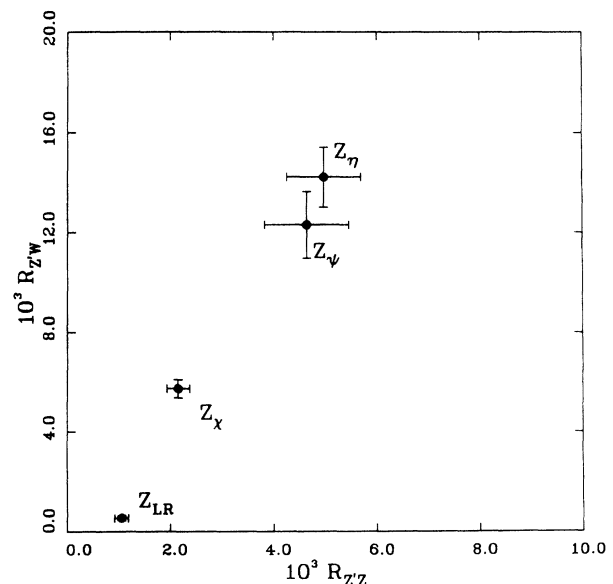


FIG. 7. $R_{Z'W}$ vs $R_{Z'Z}$ at the LHC for the χ , ψ , η , and LR models, along with the expected error bars for $M_{Z'} = 1$ TeV.

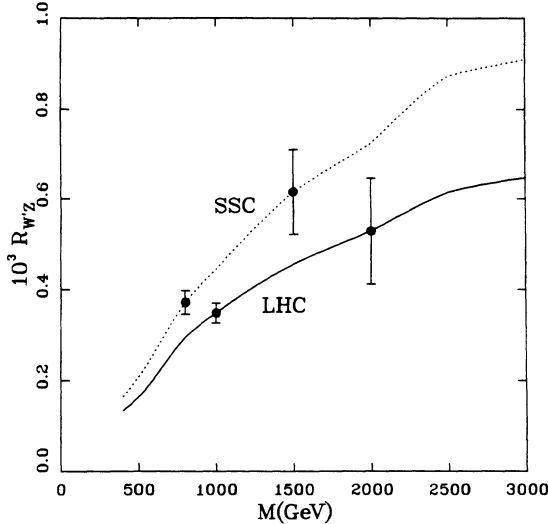


FIG. 8. $R_{W'Z}$ as a function of the W' mass for left-right-symmetric models at the LHC and SSC. The corresponding predictions for W'^{\pm} are very similar.

$\tau \rightarrow \pi\nu$, it might be possible [35] to make such measurements. The branching ratios would allow one to determine the interfamily universality in the lepton sector for the quantities $\hat{g}_{L2}^2 + \hat{g}_{R2}^2$. Other combinations of \hat{g}_{L2}^2 and \hat{g}_{R2}^2 would be probed by comparing A_{FB}^l and $r_{l\nu W}$ for $l = e$ and μ .

Nature of enhanced gauge structure. The most likely possibility for a new Z' in an extended gauge group is that it corresponds to a $U'(1)$ or other group that commutes with the standard model $[Q', T_i] = 0$. That can in principle be tested [24,28] (in the absence of Z - Z' mixing) from the ratio $r_{l\nu W}/r_{\nu\nu Z}$, where $r_{\nu\nu Z} = B(Z' \rightarrow Z\nu\nu)/B(Z' \rightarrow ll)$, which depends only on the Z' mass provided $[Q', T_i] = 0$ (see below). In enlarged gauge groups with $[Q', T_i] \neq 0$ there are additional non-Abelian contributions, while for nongauge theories (e.g., composite vectors), $r_{l\nu W}$ and also $R_{Z'W}$ may have anomalous or senseless values. Unfortunately, as will be discussed below, $r_{\nu\nu Z}$ suffers from a large standard-model background from $pp \rightarrow ZZ$ [24,27] and is thus probably unmeasurable at hadron colliders.

Z - Z' mixing. As discussed in Sec. III small Z - Z' mixing angles have a negligible effect on the $pp \rightarrow V'V$ rate. One place where mixing could be relevant for colliders is in the decay $Z' \rightarrow WW$ [16–19]. Although the rate is suppressed by the square of the mixing angle [$\propto C(M_1/M_2)^4$], the longitudinal components of the gauge bosons give an enhancement $\propto (M_2/M_1)^4$. A precise measurement of C would yield valuable information on the symmetry-breaking sector of the theory [1,20]. However, leptonic modes suffer from a serious standard-model background $pp \rightarrow WW$. The semileptonic modes have additional QCD backgrounds from $pp \rightarrow W + \text{jets}$ [18], although it may still be possible to observe the decay with appropriate cuts [19].

Another possibility [28] is to search for $Z' \rightarrow WW \rightarrow Wl\nu$ indirectly by looking for an anomalous ratio $r_{l\nu W}/r_{\nu\nu Z}$ compared to that predicted from the diagrams

in Fig. 4. However, that is not practical due to the difficulty of observing [24,27] $r_{\nu\nu Z}$.

A better approach would be to try to separate the $Wl\nu$ events due to mixing from those from rare decays directly, since they have very distinct kinematic distributions. In the Z' rest frame a majority of the rare-decay events are back-to-back fermions with invariant mass close to $M_{Z'}$ and a soft W emitted, while the mixing events consist of back-to-back W 's in the Z' rest frame. With the second W decaying hadronically one can determine the transverse mass $m_{Tl\nu}$ of the $l\nu$ in the pp center of mass. $m_{Tl\nu}$ must be $< M_W$ for the mixing events, while some 96% of the rare decays of a 1 TeV Z' have $m_{Tl\nu} > 90$ GeV at the LHC [24]. Thus, the kinematic regions of the two types of events are essentially disjoint. However, both processes have a major background from $pp \rightarrow WW$. As described below, a cut $m_{Tl\nu} \geq 90$ GeV removes this background to the rare decays $r_{l\nu W}$, but at the same time it eliminates the events due to mixing. The best prospect for probing Z - Z' mixing is therefore in future precision experiments [5] rather than hadron colliders.

Nature of gauge couplings for leptons and quarks. In the following we study the extraction of information on the gauge couplings from the three types of the proposed signals: rare decays, forward-backward asymmetry, and $V'V$ production. Assuming family universality, $[Q', T_i] = 0$, and neglecting Z - Z' mixing, the relevant quantities to distinguish different theories are the charges $\hat{g}_{L2}^u = \hat{g}_{L2}^d \equiv \hat{g}_{L2}^q$, \hat{g}_{R2}^u , \hat{g}_{R2}^d , $\hat{g}_{L2}^e = \hat{g}_{L2}^{\nu_e} \equiv \hat{g}_{L2}^l$, and \hat{g}_{R2}^e , and the gauge coupling strength g_2 . The overall scale of the charges (and g_2) depends on the normalization convention for $\text{Tr}Q'^2$, but the ratios characterize particular theories. There is little chance of ever determining the signs of the charges at hadron colliders (some information is possible from precision experiments, as is mentioned below), so we will concentrate on the four “normalized” observables,

$$\gamma_L^l \equiv \frac{(\hat{g}_{L2}^l)^2}{(\hat{g}_{L2}^l)^2 + (\hat{g}_{R2}^l)^2}, \quad (4.1)$$

$$\gamma_L^q \equiv \frac{(\hat{g}_{L2}^q)^2}{(\hat{g}_{L2}^q)^2 + (\hat{g}_{R2}^q)^2}, \quad (4.2)$$

$$\gamma_R^u \equiv \frac{(\hat{g}_{R2}^u)^2}{(\hat{g}_{L2}^u)^2 + (\hat{g}_{R2}^u)^2}, \quad (4.3)$$

$$\gamma_R^d \equiv \frac{(\hat{g}_{R2}^d)^2}{(\hat{g}_{L2}^d)^2 + (\hat{g}_{R2}^d)^2}. \quad (4.4)$$

It will also be convenient to introduce

$$\tilde{U} \equiv \gamma_R^u / \gamma_L^q, \quad (4.5)$$

$$\tilde{D} \equiv \gamma_R^d / \gamma_L^q. \quad (4.6)$$

The values of γ_L^l , γ_L^q , γ_R^u , γ_R^d , \tilde{U} , and \tilde{D} for the χ , ψ , η , and LR models are listed in Table III. It is seen that they vary significantly from model to model. In principle, all of the γ 's can be determined at hadron colliders. In practice, however, only γ_L^l and $2\tilde{U} + \tilde{D}$ can be well determined for projected LHC and SSC luminosities.

TABLE III. Values of γ_L^l , γ_L^q , γ_R^u , γ_R^d , \bar{U} , \bar{D} , and $2\bar{U} + \bar{D}$ for the χ , ψ , η , and LR ($\kappa=1$) models.

	χ	ψ	η	LR
γ_L^l	0.9	0.5	0.2	0.36
γ_L^q	0.1	0.5	0.8	0.04
γ_R^u	0.1	0.5	0.8	1.4
γ_R^d	0.9	0.5	0.2	2.6
\bar{U}	1	1	1	37
\bar{D}	9	1	0.25	65
$2\bar{U} + \bar{D}$	11	3	2.3	139

For rare decays one observes the ratios [24] $r_{f_1 f_2 \nu} \equiv B(Z' \rightarrow f_1 \bar{f}_2 V) / B(Z' \rightarrow l^+ l^-)$, where $V = W$ or Z . We always sum over $l = e, \mu$, over W^+, W^- , and over the neutrino flavors. The expressions for $r_{f_1 f_2 (W,Z)} / a_{W,Z}$ are bounded [36] to a specific range [24,28]. Here

$$a_{W,Z} \simeq \frac{\alpha}{6\pi \cos^2 \theta_W \sin^2 \theta_W} \left[\ln^2 \mu + 3 \ln \mu + 5 - \frac{\pi^2}{3} \right] \quad (4.7)$$

are kinematic factors that only depend on $\mu \equiv M_{Z,W}^2 / M_Z^2$. For $M_{Z'} = 1$ TeV, $a_Z (a_W) = 0.068$ (0.080). For example,

$$\frac{r_{ffZ}}{a_Z} = \frac{(\hat{g}_{L1}^f)^2 (\hat{g}_{L2}^f)^2 + (\hat{g}_{R1}^f)^2 (\hat{g}_{R2}^f)^2}{(\hat{g}_{L2}^f)^2 + (\hat{g}_{R2}^f)^2}. \quad (4.8)$$

One can write the leptonic r 's as

$$\begin{aligned} \frac{r_{llZ}}{a_Z} &= 0.0529 + 0.020 \gamma_L^l, \\ \frac{r_{\nu\nu Z}}{a_Z} &= 0.375 \gamma_L^l \leq 0.375, \end{aligned} \quad (4.9)$$

$$\frac{r_{l\nu W}}{a_W} = 0.77 \gamma_L^l \leq 0.77,$$

and the hadronic r 's as

$$\begin{aligned} \frac{r_{\text{had}Z}}{a_Z} &= 1.17 \gamma_L^q + 0.071 \gamma_R^u + 0.026 \gamma_R^d, \\ \frac{r_{\text{had}W}}{a_W} &= 2.31 \gamma_L^q, \end{aligned} \quad (4.10)$$

where we have used $\sin^2 \theta_W \simeq 0.23$. [We define $r_{\text{had}W,Z}$ as decays into light hadrons (W, Z) only; i.e., those including the t quark are not included.] Since γ_L^l is in the range (0,1), the expressions (4.9) are limited to a certain range. Also, one has $(r_{l\nu W} / r_{\nu\nu Z})(a_Z / a_W) = 2.05$ (so that all models satisfying $[Q', T_i] = 0$ lie on a straight line [24,28], $r_{\nu\nu Z}$ versus $r_{l\nu W}$, for a fixed value of $M_{Z'}$), and $(r_{\text{had}Z} / r_{\text{had}W})(a_W / a_Z) \geq 0.51$. These predictions follow directly from $[Q', T_i] = 0$, small Z - Z' mixing, and family universality, and any deviation would imply a breakdown of one of these assumptions. The r 's are shown for the models considered in Refs. [24,20].

The quantities in (4.9) and (4.10) in principle determine γ_L^l , γ_L^q , and $\gamma_R^u + \frac{3}{8} \gamma_R^d$. In practice, however, the dependence on the γ_R 's is very weak.

In hadron colliders the hadronic ratios $r_{\text{had}Z}$ and $r_{\text{had}W}$ suffer [24] from serious QCD backgrounds. Similarly, $r_{\nu\nu Z}$ suffers from the standard-model background $pp \rightarrow ZZ$, with one $Z \rightarrow \nu\bar{\nu}$. Even with the second Z fully reconstructed by its hadronic or charged lepton decays, the only observables are the energy E_Z and angle $\cos \theta_Z$ in the pp center of mass. For a 1-TeV Z' , for example, the signal-to-background ratio is $\simeq 10^{-2}$, as shown in Fig. 9(a). The rare-decay events have a somewhat harder spectrum, and a flatter $\cos \theta_Z$ distribution for large E_Z , but even by applying severe cuts (e.g., $\cos \theta_Z < 0.6$, $E_Z > 300$ GeV), the signal-to-background ratio is still only 10^{-1} , and one has lost most of the signal. Hence $r_{\nu\nu Z}$ is probably unobservable at hadron colliders. However, $r_{\nu\nu Z}$ and $r_{\text{had}W,Z}$ might be useful at future e^+e^- machines.

On the other hand, r_{llZ} provides a very clean signal. Unfortunately, it has a weak dependence [24] on γ_L^l due to the fact that $|\hat{g}_{L1}^l| \simeq |\hat{g}_{R1}^l|$ for $\sin^2 \theta_W \simeq 0.23$, and thus r_{llZ} serves only as a consistency check.

The backgrounds for the ratio $r_{l\nu W}$ can be eliminated with appropriate cuts. As discussed earlier, the mode with W decaying hadronically can be separated from the standard-model background from $pp \rightarrow WW$ (as well as the events due to Z - Z' mixing) by requiring [24] the transverse mass $m_{Tl\nu} \geq 90$ GeV. This cut reduces the signal only by 4% for $M_{Z'} = 1$ TeV at the LHC [Fig. 9(b)]. Events with $W \rightarrow l\nu$ may also be observable with appropriate cuts [27]. The ratio $r_{l\nu W}$ thus provides the gold-plated signal that tests the left-handed coupling of leptons γ_L^l . One expects an accuracy of (2–10)% on γ_L^l at the LHC for the specific models considered here.

The second probe is the forward-backward asymmetry. For $pp \rightarrow Z' \rightarrow l^+ l^-$,

$$A_{\text{FB}} = \frac{\left[\int_0^{y_{\text{max}}} - \int_{y_{\text{min}}}^0 \right] [F(y) - B(y)] dy}{\int_{y_{\text{min}}}^{y_{\text{max}}} [F(y) + B(y)] dy}, \quad (4.11)$$

where $F(y) \pm B(y) = \left[\int_0^{\pm 1} d \cos \theta (d^2 \sigma / dy d \cos \theta) \right]$ and θ is the l^- angle in the Z' rest frame. A_{FB} can be expressed in terms of gauge couplings as

$$A_{\text{FB}} = \frac{3}{4} (2\gamma_L^l - 1) 0.58 \frac{1 - 0.75\bar{U} - 0.25\bar{D}}{1 + 0.68\bar{U} + 0.32\bar{D}} \quad (4.12)$$

for a 1-TeV Z' at the LHC. Here the quark distribution functions of Ref. [34] were used. A_{FB} thus depends on γ_L^l , and on the combination $\simeq 2\bar{U} + \bar{D}$ of right-handed currents. A_{FB} is shown as a function of $M_{Z'}$ for various models in Fig. 10, along with the analogous A_{FB} for heavy W_R^\pm production. It is seen that the statistical errors are small enough to discriminate effectively up to $\simeq 2$ TeV, provided that good enough lepton charge identification can be achieved. A_{FB} is shown as a function of $\cos \beta$ for model (iv) in Fig. 11, and as a function of κ for the LR model (v) in Ref. [20]. Typically, one should be able to determine $2\bar{U} + \bar{D}$ to (5–10)% for $M_{Z'} \simeq 1$ TeV if γ_L^l is known independently from $r_{l\nu W}$.

The exact coefficients of \bar{U} and \bar{D} in A_{FB} depend on

$M_{Z'}$, E_{pp} , and the kinematic cuts. In principle one could separate \tilde{U} and \tilde{D} by considering A_{FB} for various ranges of y . However, we have found that this provides little additional information for the projected LHC and SSC luminosities.

The forward-backward asymmetry for $pp \rightarrow W'^{\pm} \rightarrow l^{\pm} n_l$ does not distinguish $V+A$ couplings of the W' from $V-A$. As described above, this information can be obtained from $pp \rightarrow W'Z$ and the nonobservation of $pp \rightarrow W'_R W$ and $W'_R \rightarrow Wl^+l^-$.

The third probe of Z' charges are ratios R associated with $Z'V$ production. They are of the form

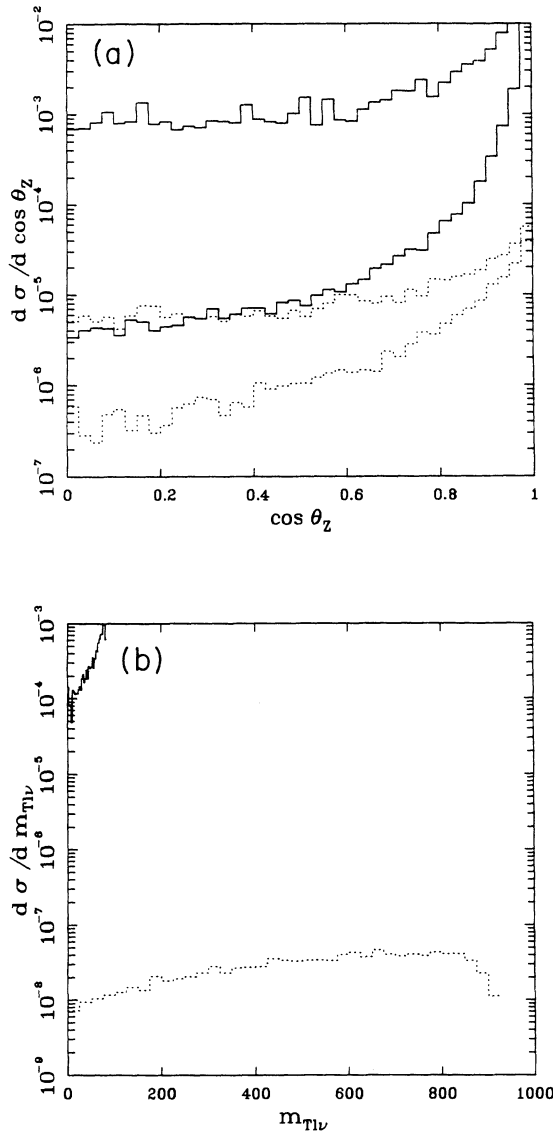


FIG. 9. (a) $\cos\theta_Z$ distribution for $pp \rightarrow ZZ$, with one $Z \rightarrow \nu\bar{\nu}$, in the standard model at the LHC (solid lines), compared with the signal for a 1 TeV $Z_\chi \rightarrow Z\nu\bar{\nu}$ (dotted lines). The upper (lower) histograms are for no E_Z cut ($E_Z > 300$ GeV). (b) Transverse mass $m_{Tl\nu}$ for $pp \rightarrow W^+W^-$, with one $W \rightarrow l\nu$, in the standard model at the LHC (solid line), compared with the signal for a 1-TeV $Z_\chi \rightarrow W^\pm l^\mp \nu$ (dotted line).

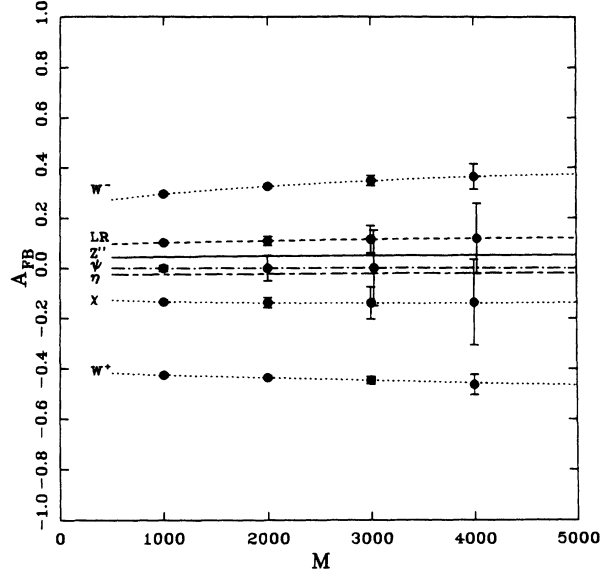


FIG. 10. A_{FB} is plotted as a function of $M_{Z'}$ at the LHC for the models described in the text.

$$R_{Z'Z} = 10^{-3} \frac{7.0 + 0.85\tilde{U} + 0.09\tilde{D}}{1 + 0.68\tilde{U} + 0.32\tilde{D}}, \quad (4.13)$$

$$R_{Z'W} = 10^{-3} \frac{22.2}{1 + 0.68\tilde{U} + 0.32\tilde{D}},$$

for a TeV Z' at the LHC. Again, the quark distribution functions of Ref. [34] were used. The numerator in the expression for $R_{Z'Z}$ has a weak dependence on \tilde{U} and \tilde{D} ; this is in part due to the fact that they are weighted by the squares of the gauge couplings of the right-handed quarks to Z , which in the standard model have small values. This in turn implies that the ratio $R_{Z'W}/R_{Z'Z}$ is usually close to the numerical constant 3.2; however, it

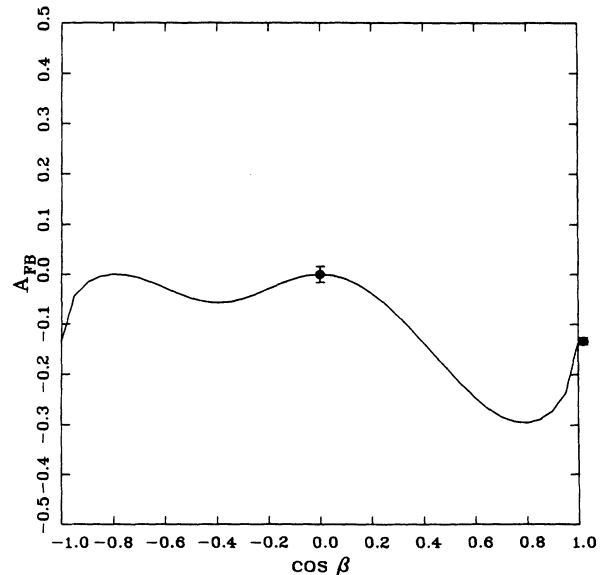


FIG. 11. A_{FB} plotted as a function of $\cos\beta$ for $M_{Z'} = 1$ TeV at the LHC.

can deviate sizably for this value in the gauge theory models with $\gamma_R^{u,d}$ large, e.g., in the left-right-symmetric model (v).

Since the ratios R are free of major standard-model and QCD backgrounds, the expressions in (4.13) provide the first clean probe to yield direct information on the couplings of *quarks* to Z' . Except in models with large \tilde{U} and \tilde{D} the R 's mainly determine the combination $2\tilde{U} + \tilde{D}$, typically with a precision of $\sim(10-20)\%$. This is the same quantity that is probed by A_{FB} (for a known γ_L^l), but the extra information provides a welcome consistency check. Again additional information to separate \tilde{U} and \tilde{D} could in principle be obtained by using appropriate y cuts, but the statistics are not adequate for this for projected luminosities. In the case of models with heavy charged gauge bosons the ratio $R_{W'V}$ would also yield information on the coupling of W' to the quarks.

One should emphasize that in the case of A_{FB} and the R 's the actual numerical coefficients in (4.11) and (4.13) depend on the quark distribution functions. Thus, while the experimental detection of these signals is clean, the actual extraction of the value of couplings crucially depends on precise knowledge of structure functions and higher-order QCD effects. The coefficients would have to be recalculated if a heavy V' were actually discovered.

We would also like to mention that it would be useful if one could measure the branching ratio $B(Z' \rightarrow q\bar{q})$. Then the ratio $\frac{1}{3}B(Z' \rightarrow q\bar{q})/B(Z' \rightarrow l^+l^-) = 2\gamma_L^q + \gamma_R^u + \gamma_R^d$ (counting all three families) could be an excellent test of the quark couplings. However, the QCD background is too large for this quantity to be easily measurable with reasonable resolutions. Thus, the ratios R and A_{FB} remain as the only tests to extract information about the quark couplings.

Thus, hadron colliders allow determination of the quantities γ_L^l and $\simeq 2\tilde{U} + \tilde{D}$ with reasonable precision for a 1-TeV Z' . From Table III, we see that these quantities are a reasonable but not total discriminant between models. This is further illustrated in Figs. 12 and 13, in which the predictions for γ_L^l and $2\tilde{U} + \tilde{D}$ are shown along with typical statistical error bars for the left-right symmetric and E_6 models, as functions of κ and $\cos\beta$, respectively. We see that the combination of γ_L^l and $2\tilde{U} + \tilde{D}$ determines κ without ambiguity within the interesting range 0.6–1. There is still a twofold ambiguity in the $\cos\beta$ value for E_6 models. The approximate symmetry around $\cos\beta \sim -0.4$ and ~ 0.8 is due to the vanishing of the couplings of the SU(5) 5-plet (10-plet) in Table I, and cannot be resolved at a hadron collider by any means that we are aware of.

For some parameter ranges, the E_6 and left-right models cannot be distinguished, as is expected since left-right models can be embedded in E_6 . This is not a major problem, however, because if a Z_{LR} is discovered directly at a hadron collider, the associated W'_R would almost certainly also be seen. For most symmetry breaking structures, the W'_R is lighter than the Z_{LR} , and the ratio $M_{W'_R}/M_{Z_{LR}}$ would be a useful probe [20].

At the end we would also like to address determination of the absolute magnitude of g_2 , which would shed light

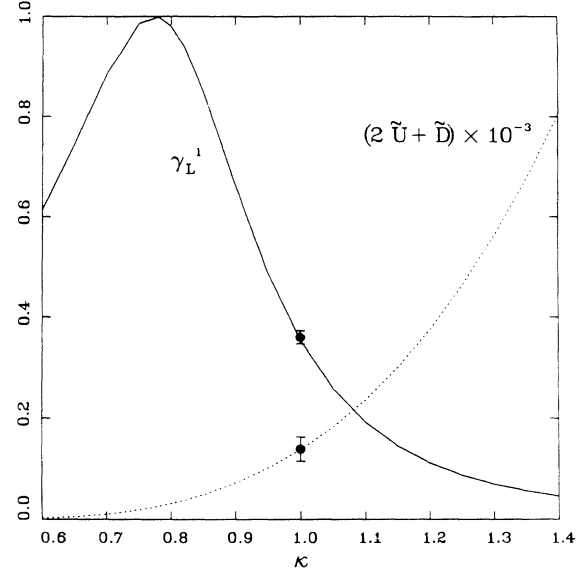


FIG. 12. γ_L^l and $2\tilde{U} + \tilde{D}$ in left-right-symmetric models (v) as a function of $\kappa = g_R/g_L$, along with typical statistical error bars.

on the nature of the spontaneous symmetry breaking in a grand unified theory [22] or left-right model [1,20]. As discussed in the Introduction, for a given theory [i.e., a given set of $\gamma_{L,R}$'s and a normalization convention for $\text{Tr}(Q')^2$] the strength of g_2 can be determined from the combination $\sigma\Gamma(Z' \rightarrow l^+l^-) \equiv \sigma B\Gamma_{\text{tot}}$, while Γ_{tot} would then allow an estimate of the fraction of Z' decays into exotic fermions and superpartners.

Interestingly, the low-energy, atomic-parity-violation experiments could also measure the change in the effective weak charge [2–5] Q_W ,

$$\Delta Q_W = -2(2Z + N)\Delta C_{1u} - 2(Z + 2N)\Delta C_{1d}, \quad (4.14)$$

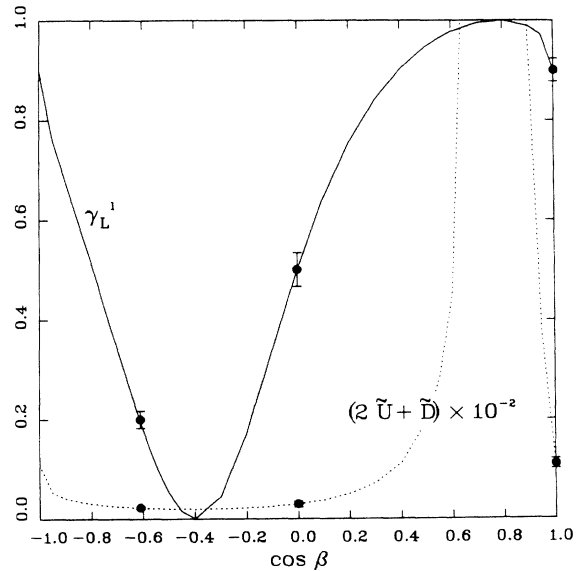


FIG. 13. γ_L^l and $2\tilde{U} + \tilde{D}$ in the general E_6 models (iv) as a function of $\cos\beta$, along with typical errors.

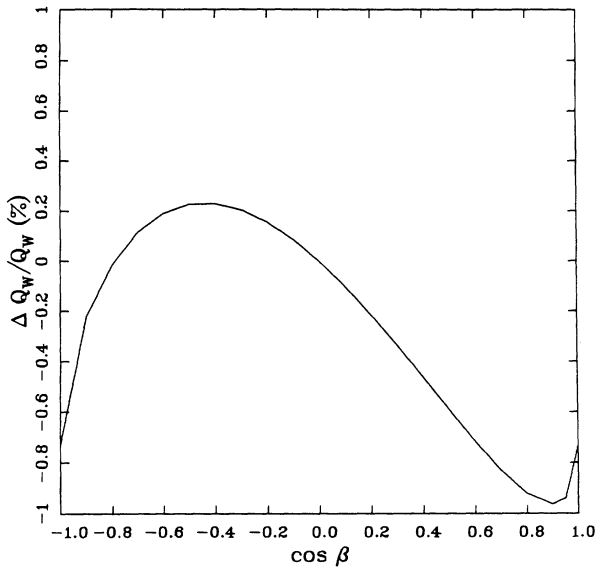


FIG.14. Fractional change (%) in the atomic-parity-violation parameter Q_W in cesium, for $M_{Z'}=1$ TeV and $\lambda_g=1$. In the LR model (v) the change $\sim -0.8\%$ depends only weakly on κ .

where Z and N refer to the atom and (when $\theta=0$):

$$\Delta C_{ii} = 2 \frac{g_2^2 M_1^2}{g_1^2 M_2^2} (\hat{g}_{L2}^i - \hat{g}_{R2}^i) (\hat{g}_{L2}^q + \hat{g}_{R2}^i), \quad (4.15)$$

for $i=u,d$. This and other precision measurements could provide an independent way to gain information about the absolute value of the coupling. The fractional shift in Q_W in cesium is shown as a function of $\cos\beta$ for a 1-TeV Z' in Fig. 14. It is seen that a precision of a few tenths of a percent would yield a rough determination of g_2 , but would not resolve the $\cos\beta$ ambiguities.

V. CONCLUSIONS

In this paper we have proposed the production cross sections for $V'V$ with $V'=W',Z'$ and $V=W,Z$ as a

probe of the nature of the gauge couplings of fermions to heavy gauge bosons at future hadron colliders. This is the third and complementary probe for the diagnostic study of such couplings, the first two being the forward-backward asymmetry [11] and the rare decays [24,26]. The rates for the production of $V'V$ are large for $M_{V'} \sim 1$ TeV and the events with V' decaying into charged leptons are clean with good diagnostics for the couplings of quarks to V' . For $M_{Z'} \sim 1$ TeV, the LHC at its projected luminosity would produce a factor of 2 more events than the SSC at its projected luminosity; the SSC would have more events for $M_{Z'} \geq 3$ TeV. For Z' the events probe the nature of the U'_1 group, while for W' one can test the $V+A$ nature of the currents and the non-Abelian $W'W'Z$ vertex.

In addition, we have presented a study of extracting information about the nature of the gauge coupling from the proposed signals. We have shown that for models with family universality, $[Q', T_i]=0$, and small $Z-Z'$ mixing there are four ratios of the squares of gauge charges that are in principle measurable at hadron colliders. In practice only two combinations, γ_L^i and $2\bar{U} + \bar{D}$, are accessible at projected luminosities, and there are several complementary measures of these. They have considerable though not complete ability to discriminate between models. Complementary information from σ_B , Γ_{tot} , W' production, $M_{W'}/M_{Z'}$, atomic parity violation, and other precision experiments should provide additional information to resolve ambiguities and to probe other aspects of the theory. Detection of such signals, and thus the diagnostic study of such gauge couplings, would clearly improve with an increased luminosity at the SSC, which would in turn provide an important window to learn more about gauge structures beyond the standard model.

ACKNOWLEDGMENT

This work was supported by the Department of Energy Grant No. DE-AC02-76-ERO-3071 and Texas National Research Commission (M.C.). We would like to thank Jiang Liu for useful discussions.

- [1] M. Cvetič and P. Langacker, Phys. Rev. D **42**, 1797 (1990).
- [2] G. Altarelli *et al.*, Phys. Lett. B **263**, 459 (1991); **261**, 146 (1991); J. Layssac, F. M. Renard, and C. Verzegnassi, Z. Phys. C **53**, 97 (1992); F. M. Renard and C. Verzegnassi, Phys. Lett. B **260**, 225 (1991).
- [3] K. T. Mahanthappa and P. K. Mohapatra, Phys. Rev. D **43**, 3093 (1991); P. Langacker, Phys. Lett. B **256**, 277 (1991).
- [4] F. del Aguila, W. Hollik, J. M. Moreno, and M. Quiros, Nucl. Phys. B **372**, 3 (1992); F. del Aguila, J. M. Moreno, and M. Quiros, *ibid.* **B361**, 45 (1991); Phys. Lett. B **254**, 479 (1991); M. C. Gonzalez-Garcia and J. W. F. Valle, *ibid.* **259**, 365 (1991).
- [5] P. Langacker and M. Luo, Phys. Rev. D **44**, 817 (1991); U. Amaldi *et al.*, *ibid.* **36**, 1385 (1987); S. Durkin and P.

- Langacker, Phys. Lett. **166B**, 436 (1986). The sensitivity of future precision experiments is discussed in P. Langacker, M. Luo, and A. K. Mann, Rev. Mod. Phys. **64**, 87 (1992).
- [6] J. C. Pati and A. Salam, Phys. Rev. Lett. **31**, 661 (1973); Phys. Rev. D **10**, 275 (1974); R. Mohapatra and J. C. Pati, *ibid.* **11**, 566 (1975).
- [7] G. Beall, M. Bander, and A. Soni, Phys. Rev. Lett. **48**, 848 (1982).
- [8] L. Wolfenstein, Phys. Rev. D **29**, 2130 (1984).
- [9] P. Langacker and U. Sankar, Phys. Rev. D **40**, 1569 (1989).
- [10] D. London and D. Wyler, Phys. Lett. B **232**, 503 (1989).
- [11] P. Langacker, R. Robinett, and J. Rosner, Phys. Rev. D **30**, 1470 (1984).
- [12] V. Barger *et al.*, Phys. Rev. D **35**, 2893 (1987).

- [13] L. Durkin and P. Langacker, *Phys. Lett.* **166B**, 436 (1986); F. del Aguila, M. Quiros, and F. Zwirner, *Nucl. Phys.* **B287**, 419 (1987); **B284**, 530 (1987); J. Hewett and T. Rizzo, in *High Energy Physics in the 1990's*, Proceedings of the Summer Study, Snowmass, Colorado, 1988, edited by S. Jensen (World Scientific, Singapore, 1989); P. Chiappetta *et al.*, in *Proceedings of the ECFA Large Hadron Collider Workshop*, Aachen, Germany, 1990, edited by G. Jarlskog and D. Rein (CERN Report No. 90-10, Geneva, Switzerland, 1990).
- [14] J. Hewett and T. Rizzo, *Phys. Rev. D* **45**, 161 (1992).
- [15] The possibilities at a 500 GeV e^+e^- collider have been studied by A. Djouadi *et al.*, DESY report, 1992, to appear in the Proceedings of the Workshop e^+e^- Collision at 500 GeV: the Physics Potential, Hamburg, Germany, 1991.
- [16] F. del Aguila, M. Quiros, and F. Zwirner, *Nucl. Phys.* **B284**, 530 (1987); P. Kalyniak and M. Sundaresan, *Phys. Rev. D* **35**, 75 (1987).
- [17] N. Deshpande, J. Gunion, and F. Zwirner, in *Experiments Detectors and Experimental Areas for the Supercollider*, Proceedings of the Workshop, Berkeley, California, 1987, edited by R. Donaldson and M. G. D. Gilchriese (World Scientific, Singapore, 1988); N. Deshpande, J. Grifols, and A. Méndez, *Phys. Lett. B* **208**, 141 (1988).
- [18] F. del Aguila, L. Ametller, R. Field, and L. Garrido, *Phys. Lett. B* **201**, 375 (1988); **221**, 408 (1989).
- [19] G. Kane and C. P. Yuan, *Phys. Rev. D* **40**, 2231 (1989).
- [20] M. Cvetič, B. Kayser, and P. Langacker, *Phys. Rev. Lett.* **68**, 2871 (1992).
- [21] M. J. Duncan and P. Langacker, *Nucl. Phys.* **B277**, 285 (1986).
- [22] R. Robinett, *Phys. Rev. D* **26**, 2388 (1982); R. Robinett and J. Rosner, *ibid.* **25**, 3036 (1982); **26**, 2396 (1982).
- [23] Note that in Ref. [24] it was erroneously mentioned that such a cross section would be at most marginal at the LHC.
- [24] M. Cvetič and P. Langacker, *Phys. Rev. D* **46**, R14 (1992).
- [25] As shown by J. Hewett and T. Rizzo, *Phys. Rep.* **183**, 193 (1989), the process $pp \rightarrow V'V'$ is too small to be useful in reasonable models because of a kinematic suppression and also smaller couplings compared to $pp \rightarrow V'V$.
- [26] T. Rizzo, *Phys. Lett. B* **192**, 125 (1987).
- [27] F. del Aguila, B. Alles, L. Ametller, and A. Grau, University of Granada Report No. UG-FT-22/92, 1992 (unpublished).
- [28] J. Hewett and T. Rizzo, Argonne National Laboratory Report No. ANL-HEP-PR-92-33, 1992 (unpublished).
- [29] T. Kinoshita, *J. Math. Phys.* **3**, 650 (1962); T. D. Lee and M. Nauenberg, *Phys. Rev.* **133**, B1549 (1964).
- [30] W. Marciano and D. Wyler, *Z. Phys. C* **3**, 181 (1979).
- [31] If the n_i is heavy, its subsequent decays may be observable and yield additional information. M. Cvetič, B. Kayser, and P. Langacker (unpublished).
- [32] R. Brown, D. Sahdev, and K. Mikaelian, *Phys. Rev. D* **20**, 1164 (1979); R. Brown and K. Mikaelian, *ibid.* **19**, 992 (1979). They also consider the related process $q_1\bar{q}_2 \rightarrow ZW$ in the standard model.
- [33] See Refs. [2–5], and P. Langacker, *Phys. Rev. D* **30**, 2008 (1984).
- [34] E. Eichten, I. Hinchliffe, K. Lane, and C. Quigg, *Rev. Mod. Phys.* **56**, 579 (1984).
- [35] J. Anderson, M. Austern, and R. Cahn, *Phys. Rev. D* **46**, 290 (1992).
- [36] The expressions must of course be modified to account for kinematic cuts.